Materials Science and Engineering A 550 (2012) 222–226

Contents lists available at SciVerse ScienceDirect

Materials Science and Engineering A

journal homepage: www.elsevier.com/locate/msea

Effect of temperature on the indentation behavior of closed-cell aluminum foam

Zhibin Li[a], Zhijun Zheng[a,*], Jilin Yu[a], Liqun Tang[b]

[a] CAS Key Laboratory of Mechanical Behavior and Design of Materials, University of Science and Technology of China, Hefei, Anhui 230026, PR China
[b] School of Civil Engineering and Transportation, South China University of Technology, Guangzhou, Guangdong 510640, PR China

ARTICLE INFO

Article history:
Received 7 March 2012
Received in revised form 11 April 2012
Accepted 18 April 2012
Available online 25 April 2012

Keywords:
Aluminum foam
Indentation
High-temperature deformation
Mechanical properties
Tear energy

ABSTRACT

Deep indentation response of closed-cell aluminum foam under different temperatures was experimentally investigated by using flat-ended and hemispherical-ended punches and compared with that under uniaxial compression. Cross-sectional views show that the deformation is roughly confined to the material directly underneath the indenter though has slight lateral spread. The plastic collapse strength, tear energy and energy absorption are found to be temperature dependent. An empirical formula incorporating indentation depth effect and test temperature effect is presented for the tear energy.

1. Introduction

Aluminum foams have drawn a great deal of attention in the past decade in automotive and aerospace industries due to their ultralight weight and other attractive mechanical characteristics, such as high specific strength and excellent energy absorption capability [1,2]. Indentation response is of interest because of the potential failure mode of aluminum foams from impacts associated with poor handling and other indentation loads intentional or unintentional in many practical applications. Thus, foams may be subjected to localized loads instead of uniform loading over an entire face. Due to the great potential of aluminum foams to be used in some extreme environmental conditions where high temperature and high stresses are involved as for example in the transpiration cooled rocket nozzles, in the cooling system of the burning chamber in gas and steam turbines and heat shielding for aircraft exhaust [1,3], it is necessary to understand their high-temperature mechanical properties. Moreover, previous studies of fully dense annealed Al alloys have shown that temperature more strongly affects the yield and flow stress behavior than strain rate [4]. It would lead to significant errors if the data under room temperature were used in numerical simulations or designs at extreme temperatures. Therefore, reliable experimental results with temperature effects are necessary.

A number of previous studies on the indentation of aluminum foams were presented [5–10]. Results showed that plastic deformation of aluminum foam was localized in the region just underneath the indenter. However, the concern of the temperature effects on the mechanical properties of aluminum foams is so far only limited to uniaxial compressions (UC). Zhou et al. [11] studied the effect of heat treatment on the compressive deformation behavior of an open-cell aluminum foam, Duocel®, using a combination of experimental investigation and digital image correlation technique. Aly [3] and Hakamada et al. [12] carried out compressive tests on a closed-cell aluminum foam, ALPORAS®, at ambient as well as elevated temperatures in order to study the difference in their behavior in terms of the foam's density and test temperature. The compressive constitutive behavior of ALPORAS® was evaluated by Cady et al. [13] under static and dynamic loading conditions as a function of temperature. The knowledge of the indentation behavior of aluminum foam at elevated temperatures is still not available.

The present study aims to present systematic results illustrating the effect of temperature on the indentation response of closed-cell aluminum foam via conducting deep indentation experiments with flat-ended and hemispherical-ended punches at temperatures ranging from 25 °C to 500 °C.

2. Materials and experiments

A commercially available closed-cell aluminum foam (supplied by Osenter Metal Composite Materials Co. Ltd., Shanghai, China) was used in the present tests, which is produced by liquid state processing using TiH_2 as a foaming agent. The foam has an average cell size of ~3 mm and a relative density of ~20%.

* Corresponding author. Tel.: +86 551 360 3044; fax: +86 551 360 6459.
E-mail address: zjzheng@ustc.edu.cn (Z. Zheng).

0921-5093/$ – see front matter © 2012 Elsevier B.V. All rights reserved.
http://dx.doi.org/10.1016/j.msea.2012.04.062

Specimens with dimensions of Φ30 mm × 60 mm were cut from a block for compressive tests, and those with dimensions of 100 mm × 100 mm × 60 mm for indentation tests. Three replicated experiments were conducted for each loading case.

The mechanical property of metallic foams depends largely on their relative density, and the variability in the plastic strength and energy absorption are related to the variance in the cell size by considering the micro mechanism of deformation in closed-cell foams [14]. In order to minimize this variability, specimens used in this experimental work were chosen from the part of a block where the cellular structure is almost homogeneous and average cell size is nearly constant. Moreover, the density of the aluminum foam used in this study was determined by use of a digital caliper to measure the dimensions of the specimens and a digital balance to determine the weight. In order to minimize the error, the length, the width and the thickness of each specimen are measured at five different positions. The density of the sample is then calculated by dividing the weight on its volume. The measured density was found to be around 0.55 g/cm^3 with a variability (defined as the standard deviation normalized by the mean value) of 8%.

An MTS810 testing system was used to carry out the tests under displacement control with a nominal rate of 0.06 mm/s. A rigid substrate support covering the entire area of the specimen was put underneath the specimen panels during the tests. Two types of axisymmetric indenter, i.e. a flat-ended punch (FEP) and a hemispherical-ended punch (SEP), with 30 mm in diameter were used.

Cell size, indenter diameter, specimen dimension and indentation depth may affect the indentation responses, so precautions have been taken to eliminate these size effects. For both types of indenter, the ratio of the indenter diameter to the average cell size is about 10. In this case no significant effect of cell size on indentation response will be noticed, according to Olurin et al. [5] and Andrews et al. [15]. Edge effects are avoided if the indentations are at least one indenter diameter away from the free edge of the foam block [2,15]. In the current study, the size of the specimens (100 mm) is larger than the above requirement (90 mm) so the edge effect on the load–displacement behavior can be negligible. According to Kumar et al. [7], if the indentation depth exceeds more than half of the thickness of specimen then the indentation response will be affected by the back support and lead to very steep behavior afterwards. In our experiments, the maximum indentation depth was 30 mm, which is just half of the specimen thickness.

For comparison purposes, uniaxial compression (UC) tests were conducted on cylindrical specimens. Compression and indentation tests were carried out at four different temperatures: 25 °C (room temperature, RT), 200 °C, 350 °C and 500 °C. The deviation from each test temperature was within 5 °C.

3. Results

3.1. Load response

Typical load–displacement curves are shown in Fig. 1. Two curves are given for every loading case indicating a good reproducibility of the experiments. The UC tests exhibit an initial elastic regime and a peak load which indicates the start of the plastic collapse of the cell walls. Crushing load becomes constant or slightly strain hardening soon after yielding under all test conditions investigated for UC. The response of FEP indentation is somewhat similar to that seen in the UC. An elastic regime is followed by an oscillating plastic regime wherein localized plastic collapse propagates from one cell band to another. However, the load for FEP indentation is significantly larger in comparison with UC at the same temperature. This is due to the fact that the indenter has to tear the cell walls at its periphery and the tearing resistance increases with increasing indentation depth *h*. Moreover, there is a continuously increasing crushed zone of densified foam underneath the indenter which requires additional force. Another distinguished feature of the FEP indentation is that the load increases linearly with the increase of displacement while the load–displacement curves for UC appear to be nearly independent of displacement in the plastic collapse regime. The load–displacement curve obtained by using the SEP is different, which does not show a distinct peak load or a marked elastic regime. The load grows continuously as the displacement increases. The oscillations in the load–displacement responses are due to repeating cycles of cell wall yield, cell band collapse and densification.

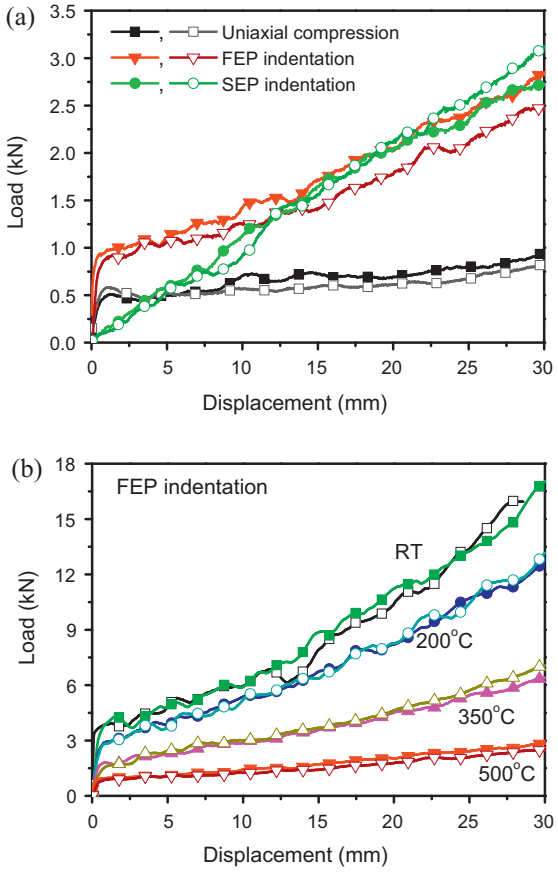

Fig. 1. Typical load–displacement curves for (a) different loading conditions at 500 °C and (b) FEP indentation at different temperatures (two curves are given for every loading case indicating a good reproducibility of the experiments).

3.2. Deformation features

The cross-sectional images of the specimens subjected to FEP and SEP indentations are shown in Fig. 2. It can be seen that the FEP indentation results in a crushed zone, which is not only concentrated in front of the nose of the indenter but also slightly spreads outwards through a truncated cone-shaped shear plug, as shown in Fig. 2a (marked with dash lines). This is possibly due to the relatively larger relative density of the foam tested. As the indentation gets deeper, the deformation zone is no longer cylindrical for FEP indentation and the size of the deformation zone becomes a little larger. This is different from that observed in the previous studies [5–8] on low density ALPORAS® foams. However, the SEP indentation results in very little lateral spreading of the crushed zone and deformation is highly localized in the region directly underneath the indenter. Moreover, although the deformation is

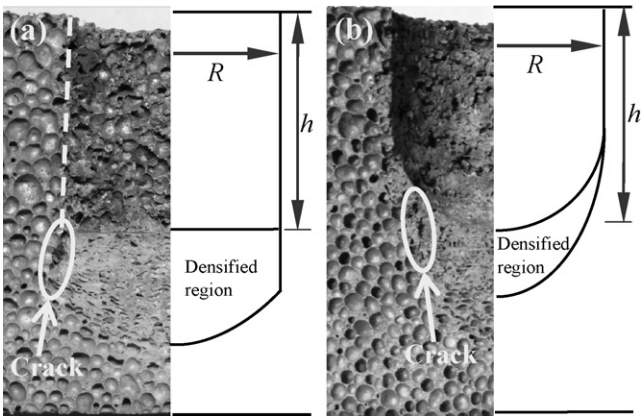

Fig. 2. Cross-sectional photographs of the specimens subjected to (a) FEP indentation and (b) SEP indentation.

extensive within the plastic zone wherein cells have been crushed, the material outside it appears to be intact. The boundary of the densified material in FEP indentation is hemispherical while the tip of the deformed zone in SEP indentation is oval-shaped and this is in general agreement with the previous numerical simulations [16,17] and experiments [5–8]. Thus, the FEP indentation produced a larger volume of compressed zone than the SEP indentation under the same indentation displacement of 30 mm, as seen in Fig. 2.

Another feature of the deformation zone for the FEP indentation is the tear lines, as can be seen from Fig. 2a (marked with dash lines). With the deepening of indentation, the densified foam gets into the undeformed foam underneath, thus tear lines generate and extend ahead of the indenter. Similar mechanism was observed by Ramachandra et al. [6] on ALPORAS® foam. However, it was observed that the tear lines are not perpendicular to the vertical axis of the indenter (marked with oval outlines). Much shorter tear cracking was found in the case of SEP indentation, which is also not perpendicular to the axis of indentation. In both cases, a circumferential densification of the foam developed along the perimeter and at the bottom of the indenter, as shown in Fig. 2.

For both indentation cases with different test temperatures, no significant difference either in deformation shape or in macrostructure morphology was observed. Moreover, with respect to the tear line length, no significant difference could be found among the specimens tested at different temperatures. However, quantitative analysis of the oscillations of the tear line length with respect to test temperature is impractical because of the large cell size of the foam.

4. Discussion

4.1. Plastic collapse strength

Variation of the plastic collapse strength (corresponding to the first peak load, which reflects the initiation of the cell band collapse) with the test temperature for both UC and FEP indentation is plotted in Fig. 3a, in which T_m = 660 °C is the melting temperature of the solid material from which the cell walls of the foam are made. It deserves noting that the data represented in this plot is the average of three or more tests and the error bars denote the standard deviations of the data. It is calculated that the variability in plastic collapse strength both for UC and FEP indentations is between 2% and 5%. This shows a good reliability of the foam used.

Fig. 3a indicates that the yield strength of the aluminum foam studied depends strongly on the test temperature. Decreasing from ~2.50 MPa at room temperature to ~0.78 MPa at 500 °C, nearly a 70% reduction in yield strength was found in UC. A similar effect of

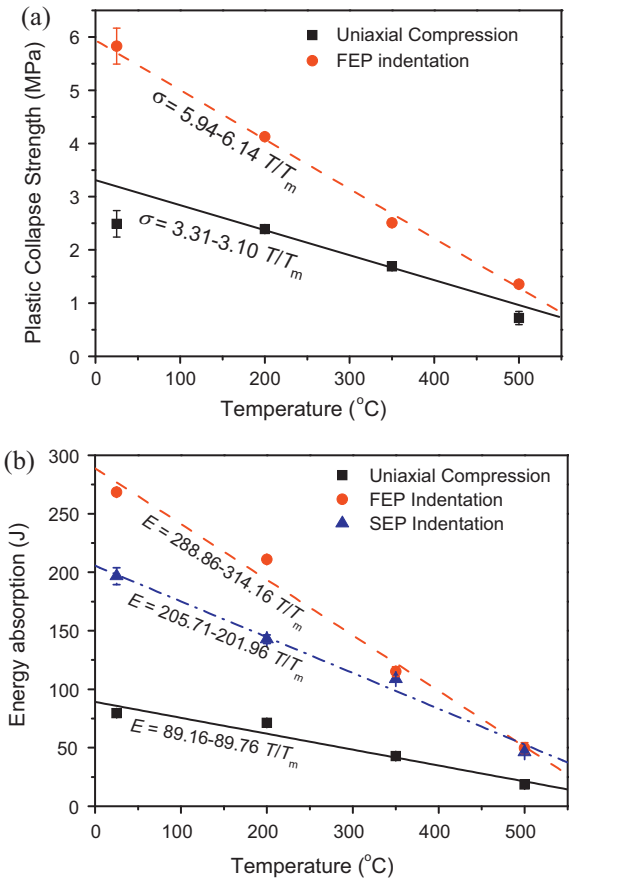

Fig. 3. Variation of (a) the plastic collapse strength and (b) the energy absorption as functions of test temperature (the error bars denote the standard deviations in replicated experiments).

temperature on the plastic collapse strength was seen in FEP indentation tests as shown also in Fig. 3a. The plastic collapse strength exhibits a more pronounced decrease, i.e. from ~5.83 MPa at 25 °C to ~1.35 MPa at 500 °C, a 77% change. For the range of temperatures tested, the plastic collapse strengths in both indentation cases decrease almost linearly with the elevation of test temperature. This is coincident with the results obtained by Aly [3] who described the elevated temperature responses of ALPORAS® foam. This temperature dependency of the aluminum foam is thought to reflect the temperature dependence of the pre-existing defect substructure and stored dislocations formed during the manufacturing process [18], and the softening effect observed with increasing temperature is related to the sliding of the grain boundaries of aluminum foams. With increasing temperature, the plastic collapse strengths of the aluminum foam loaded under UC and FEP indentation tend to converge. This suggests that for aluminum foam loaded by FEP, the relative contribution of the compression resistance to the plastic collapse strength enhanced at high temperature, in comparison with the tearing resistance.

4.2. Energy absorption

The effect of temperature on energy absorption, E, of aluminum foam is plotted in Fig. 3b for both the FEP and SEP indentations. The value of E is calculated from the area under the force-displacement curve up to an indentation displacement of 30 mm and the results obtained from UC with varying temperatures are also presented in Fig. 3b for comparison purpose. The variability measured in energy absorption of the aluminum foam under all three loading

conditions is similar to that seen for plastic collapse strength, which indicates a good reliability of the aluminum foam used in this study just as mentioned before.

As shown in Fig. 3b, E decreases with increasing T in all three cases but with different slopes. Plastic collapse in the closed-cell aluminum foam occurs due to the bending of cell walls and the stretching of cell faces. With increasing test temperature, the magnitude of the load in the plastic regime decreases and hence the energy absorption decreases [12,13].

For similar test temperature, the energy absorption is highest for the FEP indentation followed by the SEP indentation and then the UC. As the test temperature increases and approaches to the melting point, the energy absorptions of UC, SEP and FEP indentations tend to converge.

4.3. Tear energy

The total force required for FEP indentation is the sum of F_c, which is the force needed for crushing the foam underneath the indenter, and F_t, the force required to tear the cells along the periphery of the indenter [5], that is

$$F_{FEP} = F_c + F_t = \pi R^2 \sigma_p + 2\pi R\Gamma, \tag{1}$$

where R is the radius of the indenter, σ_p the compressive plateau strength of the aluminum foam, and Γ the tear energy per unit newly created area. F_c can be obtained from the UC tests and is equal to the plastic collapse strength of the foam times the cross sectional area. However, as the size of the extended deformation zone is so small that it contains only one or two cell bands, and due to the large cell size of the foam, it is not yet possible to make a quantitative assessment of the variation of extended deformation zone. Thus, the effect caused by this extended deformation zone was neglected in the calculation of present study and surely it needs further investigation. Therefore, it can be deduced that the difference between the plastic collapse strength of FEP indentation and UC is a measure of Γ. From the experimental data obtained in this work, F_t is found to increase linearly with the indentation depth h and this is in agreement with the conclusions of [8]. Also, Γ compares favorably with the mode I steady state fracture energies reported for ALPORAS® foam [16,19]. McCullough et al. [19] have investigated the origins of the observed R-curve behavior for metal foams and the micro-mechanisms of crack initiation and propagation in closed-cell aluminum-based foams and found that the fracture of metallic foams involves a fully developed fracture process zone where localized yielding, micro-cracking ahead of the crack-tip and crack bridging in the wake of the crack occur. The length of this fracture process zone can be as much as 7–8 cell diameters. Markaki and Clyne [16] suggested that the crack extension in the metallic foams occurs by a sequential renucleation of cracks across intervening tough metal ligaments. Close examination of the tear cracks emanating ahead of the tip of the indenter does indicate a fracture process zone [8], which is consistent with the observations made by Markaki and Clyne. This helps to rationalize the increase in tear energy as the depth of indentation increases because additional energy is required to break these bridges that connect the crushed zone to that surrounding it. Since the size of the crushed zone underneath the indenter increases with increasing depth of indentation, a gradual and steady increase in the tear energy can be anticipated.

Moreover, examination of Fig. 3a where plastic collapse strength for UC and FEP are plotted hints that Γ is strongly dependent on test temperature. From the experimental data obtained in this work, value of Γ extracted at $h = 0$ mm is estimated to be 25.04 N/mm at 25 °C, 13.02 N/mm at 200 °C, 6.13 N/mm at 350 °C and 4.25 N/mm at 500 °C. That is to say, Γ depends on test temperature T and also

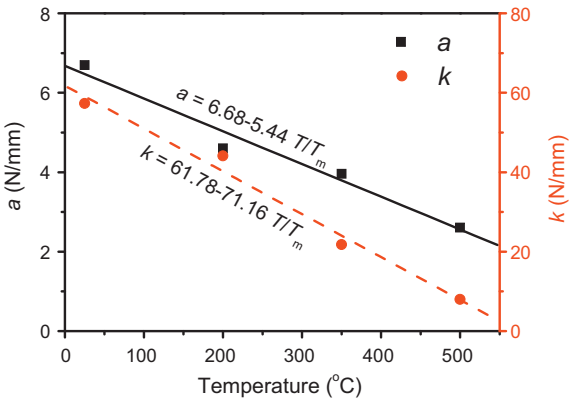

Fig. 4. Variation of coefficients a and k as functions of test temperature.

varies with indentation depth h. Then, Γ may be estimated from the following relation

$$F_t = F_{FEP} - F_{UC} = 2\pi R \cdot \Gamma(h, T). \tag{2}$$

Examination of Fig. 1 suggests an obvious linear relationship between Γ and h for each value of temperature T, which is assumed to be simply expressed as

$$\Gamma = a + k \cdot \frac{h}{R}, \tag{3}$$

where a and k are fitting parameters and change with the test temperature T. The values of a and k extracted from these fits are plotted as functions of T in Fig. 4.

As seen from Fig. 4, the values of a and k both decrease linearly with increasing T. This indicates that the plane-strain tear energy Γ changes with the test temperature linearly. Hence, it appears appropriate to assume that the tear energy Γ is related to the indentation depth h and test temperature T by

$$\Gamma(h, T) = \Gamma_0 \left(1 - \frac{\alpha T}{T_m}\right) + \Gamma_h \left(1 - \frac{\beta T}{T_m}\right) \cdot \frac{h}{R}, \tag{4}$$

where Γ_0 is the initial tear energy at $T = 0$ °C and $h = 0$ mm, Γ_h is a displacement-dependent factor, and α and β are dimensionless temperature-dependent factors. In this study, $T_m = 660$ °C and $R = 15$ mm. Other parameters can be obtained as $\Gamma_0 = 6.68$ N/mm, $\Gamma_h = 61.78$ N/mm, $\alpha = 0.82$ and $\beta = 1.15$ after fitting the relationship to the measured data in Fig. 4. Furthermore, the estimated value of Γ at room temperature for $h = 0$ mm is ~6.47 N/mm, agrees reasonably well with the value of ~7.45 N/mm reported by Olurin et al. [5] and is comparable with the value of ~9.10 N/mm obtained by Ramachandra et al. [6] for ALPORAS® foam (average cell size = 4.5 mm, relative density = 8%) at room temperature.

5. Conclusions

Deep indentation experiments of a closed-cell aluminum foam show that the plastic collapse strength, tear energy and the energy absorption characteristics are temperature dependent. The FEP indentation deformation is not only confined to the material directly underneath the indenter but also has some lateral spread, though slight. However, difference in the deformation morphology of specimens indented at various test temperatures was hardly ever observed. There is a gradual decrease in the plastic collapse strength as well as the energy absorption with increasing test temperature. As the test temperature increases, the plastic collapse strengths under FEP indentation and UC tend to converge. The tear energy per unit area is found to be dependent on test temperature and is a function of the indentation depth. Thus, an empirical equation

is proposed by fitting to the experimental results of the closed-cell aluminum foam and can be used to study the indentation of aluminum foam at various temperatures.

Acknowledgments

The research reported herein is supported by the National Natural Science Foundation of China (Project no. 90916026), the Chinese Academy of Sciences (Grant no. KJCX2-EW-L03) and the National Key Technology R&D Program of China (2009BAG12A01-B02-2), which are gratefully acknowledged.

References

[1] L.J. Gibson, M.F. Ashby, Cellular Solids: Structure and Properties, Cambridge University Press, Cambridge, 1997.
[2] M.F. Ashby, A.G. Evans, N.A. Fleck, L.J. Gibson, L.W. Hutchinson, H.G. Wadley, Metal Foams: A Design Guide, Butterworth-Heinemann, Oxford, 2000.
[3] M.S. Aly, Mater. Lett. 61 (2007) 3138–3141.
[4] J.E. Hockett, Trans. Metall. Soc. AIME 239 (1967) 969–976.
[5] O.B. Olurin, M.F. Ashby, N.A. Fleck, Scr. Mater. 43 (2000) 983–989.
[6] S. Ramachandra, P.S. Kumar, U. Ramamurty, Scr. Mater. 49 (2003) 741–745.
[7] P.S. Kumar, S. Ramachandra, U. Ramamurty, Mater. Sci. Eng. A 347 (2003) 330–337.
[8] U. Ramamurty, M.C. Kumaran, Acta Mater. 52 (2004) 181–189.
[9] K. Mohan, T.H. Yip, I. Sridhar, H. Seow, J. Mater. Sci. 42 (2007) 3714–3723.
[10] G. Lu, J. Shen, W. Hou, D. Ruan, L.S. Ong, Int. J. Mech. Sci. 50 (2008) 932–943.
[11] J. Zhou, Z. Gao, A.M. Cuitino, W.O. Soboyejo, Mater. Sci. Eng. A 386 (2004) 118–128.
[12] M. Hakamada, T. Nomura, Y. Yamada, Y. Chino, Y.Q. Chen, H. Kusuda, M. Mabuchi, Mater. Trans. 46 (2005) 1677–1680.
[13] C.M. Cady, G.T. Gray III, C. Liu, M.L. Lovato, T. Mukai, Mater. Sci. Eng. A 525 (2009) 1–6.
[14] U. Ramamurty, A. Paul, Acta Mater. 52 (2004) 869–876.
[15] E.W. Andrews, G. Gioux, P. Onck, L.J. Gibson, Int. J. Mech. Sci. 43 (2001) 701–713.
[16] A.E. Markaki, T.W. Clyne, Acta Mater. 49 (2001) 1677–1686.
[17] P.R. Onck, MRS Bull. 28 (2003) 279–283.
[18] P.S. Follansbee, High Strain Rate Deformation in FCC Metals and Alloys, Marcel Dekker Inc., New York, 1986.
[19] K.Y.G. McCullough, N.A. Fleck, M.F. Ashby, Acta Mater. 47 (1999) 2331–2343.